Accepted Manuscript

Densely Packed Matrices as Rate Determining Features in Starch Hydrolysis

Bin Zhang, Sushil Dhital, Michael J. Gidley

PII: S0924-2244(15)00024-2

DOI: 10.1016/j.tifs.2015.01.004

Reference: TIFS 1617

To appear in: *Trends in Food Science & Technology*

Received Date: 8 November 2014

Revised Date: 12 January 2015

Accepted Date: 18 January 2015

Please cite this article as: Zhang, B., Dhital, S., Gidley, M.J., Densely Packed Matrices as Rate Determining Features in Starch Hydrolysis, *Trends in Food Science & Technology* (2015), doi: 10.1016/j.tifs.2015.01.004.

Densely Packed Matrices as Rate Determining Features in Starch Hydrolysis

*Bin Zhang, Sushil Dhital, and Michael J. Gidley**

ARC Centre of Excellence in Plant Cell Walls, Centre for Nutrition and Food Sciences, Queensland Alliance for Agriculture and Food Innovation, The University of Queensland, St. Lucia, Brisbane, QLD 4072, Australia

* Corresponding author.

Phone: +61 7 3365 2145; Fax: +61 7 3365 1177. Email address: m.gidley@uq.edu.au (M. J. Gidley)

Abstract

To aid in the design of starch-containing foods with slow and/or incomplete digestion in the upper gastrointestinal tract, the starch structural factors which control the rate of action of alpha-amylase are reviewed. It is concluded that local starch molecular density has the major influence on amylase digestion kinetics, and that density sufficient to either limit enzyme binding and/or slow down catalysis can be achieved by either crystallization or dense amorphous packing.

Keywords: enzyme-resistant starch; digestion rate; amorphous matrices; amylase; starch processing

1 Introduction

Starch, a major digestible carbohydrate in human diets, is synthesised in a condensed semi-crystalline granular form by the ordered packing of two hydrophilic glucose polymers (amylose and amylopectin) during photosynthesis. It has a complex hierarchical structure, which can be described by at least four levels of organization (i.e., molecular, lamellae, growth ring, and granular levels), ranging in length scale from nanometer to micrometer. Several detailed comprehensive reviews (J-L Jane, 2006; Le Corre, Bras, & Dufresne, 2010; Oates, 1997; Tester, Karkalas, & Qi, 2004) and many research articles (Cheetham & Tao, 1998; Cooke & Gidley, 1992; Gallant, Bouchet, & Baldwin, 1997; Gidley & Bociek, 1985; J. -L. Jane, et al., 1999) on the heterogeneous organized structures of granular starch have been published.

The rate, extent, and location of starch digestion in the small intestine are controlled by intrinsic (e.g., passage rate and multiple enzyme interactions in small intestine, hormonal control, current health status) as well as starch or food structure factors. The undigested starch fraction which exits from the small intestine is defined as resistant starch (RS), and passes to the large intestine where it functions as a prebiotic for bacterial fermentation (Englyst, Kingman, & Cummings, 1992). The undigested starch entering the colon also lowers the calorific value of foods (the energy derived by the host from microbial fermentation being only about 30% of that from mammalian enzyme digestion) (Englyst & Macfarlane, 1986), as well as reducing the glycemic load and insulin responses, associated with reduced risk of developing type II diabetes, obesity, and cardiovascular disease (Behall & Hallfrisch, 2002; Brand-Miller, Holt, Pawlak, & McMillan, 2002). Fermentation of RS into short-chain fatty acid (acetate, propionate, and especially butyrate) in the colon is reported to protect colonic cells from DNA damage and reduce the risk of colon cancer (Topping, et al., 2008; Van Munster, Tangerman, & Nagengast, 1994). These health benefits have stimulated interest in both the quantity and quality of starch necessary to maintain the state of good health of an individual.

Study of starch digestion in human subjects is often expensive, ethically constrained, resource intensive, and needs to take individual diversity into account. Therefore, resistant starch is most commonly measured by *in vitro* methods that simulate *in vivo* conditions of starch digestion and referred to as 'enzyme-resistant starch (ERS)' (Chanvrier, et al., 2007) to recognize that in vitro methods cannot predict the amount of starch that reaches the large intestine as there are variable host factors which determine this as well as properties of the starch / food.

Based on their origins, ERS have been classified into four categories: (1) physically inaccessible starch; (2) native granular (B- or C-type polymorph) starch; (3) retrograded starch; (4) chemically modified starch (Englyst, et al., 1992). Recently, starch-lipid complex was proposed to be a new type of ERS (Ai, Hasjim, & Jane, 2013; Hasjim, et al., 2010; B. Zhang, Huang, Luo, & Fu, 2012). This traditional classification implies that ERS is a thermodynamically defined physical entity. However considering the complexity of starch hydrolysis, recent evidence suggests that ERS can be better expressed as a kinetic phenomenon. In this way (physiological) resistant starch is understood as that fraction of starch which has not had sufficient time to be digested in the small intestine, rather than being completely resistant to amylolysis (with the possible exception of highly chemically-modified starches).

Understanding factors that influence the kinetics of starch hydrolysis requires identification of relevant rate limiting steps. It has recently been proposed that there are two types of rate-limiting steps, namely (i) barriers that slow down or prevent access/binding of enzyme to starch or (ii) structural features that slow down or prevent amylase action (after initial binding) (Dhital, Warren, Butterworth, Ellis, & Gidley, 2014): Intact plant tissues, whole grains and complex food products are perhaps the best representatives of an ERS material caused by barriers. In these cases, starch is encapsulated by dietary components such as proteins, lipids and plant cell walls, which restrict

enzyme diffusion and hence access to starchy substrate. However, it is not only physical barriers which can limit binding, as the surface of certain granules (e.g. potato) show less binding of fluorescently-labeled amylase than maize starch granules (Dhital, Warren, Zhang, & Gidley, 2014) despite the surfaces of both being dominated by starch polysaccharides; indeed maize starch has more surface proteins and lipids than potato starch. This suggests that the supramolecular structure at exposed surfaces of B- or C- polymorphic starch granules is effectively a hard outer shell and acts as a barrier to limit rate-limiting binding of digestive enzymes, and account for its relatively resistant nature. Therefore, barriers which make binding rate-limiting and lead to ERS character are often found in unprocessed foods such as intact plant tissue, whole or partly milled grains and seeds, raw B-type starch etc.

Similarly, after initial binding, starch structural features such as chemical structure and local molecular density are likely to control the digestion kinetics of starch as these can hinder adoption of enzyme conformations that lead to productive hydrolysis. Examples of chemical structures leading to ERS character include α-limit dextrin (only resistant to α-amylase, not brush-border sucrose/isolmaltase or maltase/glucoamylase), pyrodextrin, chemical modified starches (Ao, et al., 2007; Bai, Cai, Doutch, Gilbert, & Shi, 2014; B. Zhang, Dhital, Flanagan, & Gidley, 2014; B. Zhang, et al., 2011). The currently accepted mechanism for the enzymatic resistance of this sub-category is that either the (introduced) branched glucan structures (e.g., α-limit dextrin, octenylsuccinate starch) or formation of atypical linkages (e.g., dextrinization) render the α-1,4 glucosidic linkages adjacent to the branch points inaccessible to amylase. A further category of the physical state of starch which can affect starch digestion rates is matrices/molecules with high local molecular density. Examples include some processed starches, including retrograded starch, starch-lipid complex, and some specific species/conditions (examples will be discussed later in this review). From the point view of food engineering, most starch-based foods are processed before consuming, and become less ordered

and more accessible to enzyme in most cases after processing. However, the digestibility of processed starch is not always higher than that of (densely-packed) granular starch. Parchure and Kulkarni (1997) reported that the ERS contents of rice and waxy amaranth starch subjected to pressure cooking were increased, compared to those of native starches.

Although much information is available on factors which impact on *in vitro* digestibility such as starch characteristics, modification, encapsulation (Oates, 1997; Singh, Dartois, & Kaur, 2010; Thompson, 2000), to the best of our knowledge, nothing similar has been summarized for ERS from densely packed food matrices (particularly for weakly- or non-crystalline forms). This review will focus on the role of local molecular density on starch digestion kinetics, with the principle being that density sufficient to either prevent/limit binding and/or slow down catalysis can be achieved by either re-crystallization or dense amorphous packing. We also briefly discuss enzyme interactions and data interpretation in commonly used *in vitro* starch digestion models, as this impacts on the characterization of the role of dense packing on starch amylolysis.

2 Starch digestion in vitro: Enzyme interaction and data interpretation

Resistant starch is defined as the sum of starch and products of starch degradation not absorbed in the small intestine of healthy individuals, and supposed to be predicted by physiological techniques (Champ, 2004). Although several *in vivo* techniques such as ileostomy and intestine intubation have been accepted as a reliable and direct method and performed earlier for the study of carbohydrates and starch digestion (Andersson, 1992; Champ, 2004; Englyst & Cummings, 1985), *in vivo* models are expensive, ethically constrained, and specialized to nutritional or clinical study. *In vivo* trials typically use precisely controlled and repetitive meals, whereas humans are used to diverse diets so it is difficult to study a human diet in a well-controlled way to predict health outcomes (Gidley, 2013). The drawbacks also include that limited information is available for understanding the mechanism of

food structural changes during the digestion time course. *In vitro* methods simulating various aspects of the complex human digestion environment are widely used to study the gastro-intestinal behaviour of food under relatively simple conditions and suitable for mechanistic studies and hypothesis building for food scientists.

2.1 Starch digestion in vitro: Enzyme interaction

As a biochemical mimic of *in vivo* conditions, *in vitro* study of starch digestion is normally carried out using two kinds of enzyme: porcine pancreatic or human salivary α-amylase, and fungal amyloglucosidase. The reason for the use of (excess) amyloglucosidase as a final step to convert all end products of α-amylase action to glucose is that mucosal α-glucosidases extracted from animal models are not yet available commercially, and fungal amyloglucosidase has similar functionality. The rate of enzymatic action is very dependent on conditions such as temperature and pH, although they occur generally at the optimal pH of ~5 and at temperatures around 37 °C. In this section, the structure of digestive enzymes and the nature of interaction between α-amylase and amyloglucosidase are briefly reviewed.

α-Amylases (α-1,4 glucan-4-glucanohydrolase, EC 3.2.1.1) comprise different kinds of enzymes from animals, plants, and microbes. In mammals, α-amylases are produced mostly by salivary glands and the pancreas. α-Amylases hydrolyze starch by an endo-action at inner α-1,4 linkages of starch molecules, and their products have α-configuration at the anomeric carbon of the newly produced reducing end. However, α-amylases from different sources have different product specificities, which are due to differences in the length, folding and amino acid sequences of the enzyme protein (Robyt & French, 1967). Human salivary and porcine pancreatic α-amylases, two commercial α-amylases commonly used for *in vitro* starch digestion, show similar 3D structures from X-ray crystallography (Gilles, Astier, MarchisMouren, Cambillau, & Payan, 1996; Ramasubbu, Paloth,

Luo, Brayer, & Levine, 1996). Either human salivary or porcine pancreatic α-amylase has three structural domains, about 5 nm in diameter. The domain A has a structure consisting of an eight-stranded alpha/beta barrel that contains the important active site residues (Buisson, Duee, Haser, & Payan, 1987). Domain B, protruding between beta strand 3 and alpha helix 3, probably plays a role in maintaining protein conformation and Ca^{+} binding. The function of the C-domain is not known, but mutations in the C domain of the α-amylase from *Bacillus stearothermophilus* suggest that it is involved in enzyme activity (Holm, Koivula, Lehtovaara, Hemminki, & Knowles, 1990).

Human salivary and porcine pancreatic α-amylases also show similar actions on starch (Hizukuri, 2006). They hydrolyze starch to soluble oligosaccharides (G2 (maltose), G3 (maltotriose), G4 (maltotetraose)) and α-limit dextrins that have one or two α-1,6 linkages. Robyt and French (1970) postulated that porcine pancreatic α-amylase has five D-glucose binding subsites and that the catalytic groups are located between the second and third subsites from the reducing-end subsite. This hypothesis has been confirmed by the 3D domain architecture deduced from X-ray crystallography (Buisson, et al., 1987). However, human salivary α-amylase has six D-glucose binding subsites, with catalytic groups located between the second and third subsites (Kandra & Gyemant, 2000). Glucose is a very minor product of α-amylase digestion. Only G3 and G4 can be slowly hydrolyzed into maltose and glucose after prolonged incubation by a subsidiary site (Robyt, 1986). α-Amylases have a high degree of multiple-attack hydrolysis pattern, with an average of seven hydrolytic cleavages occurring per productive encounter for the porcine pancreatic α-amylase, and three for the human salivary α-amylase (Abdullah, French, & Robyt, 1966; Robyt & French, 1967).

Another widely used starch degradation enzyme is amyloglucosidase (often called glucoamylase, EC 3.2.1.3, 8 – 10 nm in size), usually from *Aspergillus niger* (AMG-I). It can produce β-D-glucose

from the non-reducing ends of starch chains by exo-hydrolysis of both α-1,4 glycosidic linkages and, at a slower rate, α-1,6 glycosidic linkages (Weill, Burch, & Vandyk, 1954). The specific activity towards the α-1,6 linkage is only 0.2% of that for the α-1,4 linkage (Norouzian, Akbarzadeh, Scharer, & Young, 2006). Only AMG-I contains an N-terminal starch-binding domain (which is essential for the enzyme to hydrolyze granular starches) that is distinct from the C-terminal catalytic domain (active site) present in AMG-I, II and III (Takahashi, Kato, Ikegami, & Irie, 1985). Recent studies indicate that the starch-binding domain not only binds onto starch, but also disrupts double helical structures and enhances the rate of hydrolysis (Morris, Gunning, Faulds, Williamson, & Svensson, 2005; Sorimachi, LeGalCoeffet, Williamson, Archer, & Williamson, 1997). It was postulated that amyloglucosidase from *Aspergillus niger* has seven subsites for binding near the active site, and its catalytic site is located between subsites 1 and 2 (Swanson, Emery, & Lim, 1977). Moreover, the subsites possess variable affinities: the affinity of the first subsite is very low, whereas subsite 2 has the highest affinity and the affinity of the individual sites decreases from subsite 3 to 7 (Hiromi, Nitta, Numata, & Ono, 1973). Amyloglucosidase has a multi-chain hydrolysis mechanism, i.e., after the glycosidic bond is cleaved by amyloglucosidase, the remaining starch chain must dissociate and leave the active sites before glucose can leave (Robyt, 2009). The active sites of the amyloglucosidase are 'pocket like', which ensure that only a single, β-conformational glucose can be produced.

The conventional view of starch digestion is that α-amylase is the limiting digestive enzyme that determines overall digestion rate. This is indeed the case for granular starch digestion: α-amylase supplies new substrates for amyloglucosidase by endo-wise splitting of large molecules (Fujii, Homma, & Taniguchi, 1988; B. Zhang, Dhital, & Gidley, 2013). However, it was recently found that the α-amylase and amyloglucosidase have antagonistic effects in digestion of cooked starch, which was ascribed to the less efficient digestion of low molecular weight oligomers (products from α-

amylase hydrolysis) by amyloglucosidase (B. Zhang, et al., 2013). Similarly, the mucosal α-glucosidases secreted in intestinal villus do not simply passively convert the end products of α-amylase digestion (i.e., malto-ologosaccharides) to absorbable glucose, but are capable of acting directly on polymeric starch (Dhital, Lin, Hamaker, Gidley, & Muniandy, 2013; Lin, et al., 2012). Therefore, the interdependence between human α-amylase (including salivary amylase and two forms of pancreatic amylase) and mucosal α-glucosidases need to be further investigated and taken into account when predicting the digestion rate/extent of starch with different physical structures.

2.2 Starch digestion in vitro: Kinetic data interpretation

Many starch digestion processes are heterogeneous reactions, involving an interaction between solid substrate (e.g.., starch granules, food particles) and soluble enzymes. Although the starch can be gelatinized /processed, it seldom forms a true solution, and this structure is greatly influenced by the botanical source and previous processing history. Individual particles e.g. granular starches or processed starches vary in their response to enzymatic susceptibility (Al-Rabadi, Torley, Williams, Bryden, & Gidley, 2011; Dhital, Shrestha, & Gidley, 2010), and what behaves as resistant starch in one person may not behave the same way in another (Englyst, Kingman, Hudson, & Cummings, 1996), presumably because of differences in enzyme secretion levels, passage rates etc. For a given starch sample, only the mean value of digestion rate/extent for whole populations of particles can be measured under defined experimental conditions and enzyme concentration. Kinetic models and data interpretation for evaluating the rate of *in vitro* starch digestion are summarized below, including the classical Michaelis-Menten (M-M) kinetics more focusing on the initial rate and the first-order kinetics for prolonged hydrolysis.

2.3.1 Michaelis-Menten kinetics

The classical M-M kinetics is only appropriate for the initial stages of amylase digestion of starches

(typically up to ~20 min), as represented as following scheme:

$$E + S \underset{k_{-1}}{\overset{k_1}{\rightleftharpoons}} ES \overset{k_2}{\Rightarrow} E + P$$The enzyme (E) and substrate (S) first combine to give an enzyme-substrate complex (ES). Then the chemical processes take place in a second step to break down ES and produce product (P) with a first-order catalytic constant k_{cat} (also called k_2 or the turnover number). It is found experimentally that the initial rate (v) of enzyme reaction on starch can be calculated by the M-M equation using three standard assumptions: (a) The enzyme concentration in the reactions is small relative to the substrate concentration; (b) Only initial rate conditions are considered. Thus, there is very little accumulation of P, and the formation of ES from E + P is negligible; (c) Steady-state assumption. The rate of breakdown of ES equals the rate of formation of ES (Menten & Michaelis, 1913).

$$v = \frac{k_{cat} E_o S}{K_m + S}$$

where k_{cat} is catalytic constant, E_0 is the total enzyme concentration, K_m is the M-M constant which is equivalent to $(K_{-1}+K_2)/K_{+1}$, and S is the initial substrate concentration. The V_{max} is the maximum rate of the reaction, which equivalent to k_{cat} times E_0. The velocity of liberation of reducing sugars as a function of only initial (low) starch concentrations can be described through a simple M-M equation, because product inhibition and substrate exhaustion might cause the reaction velocity to decay with prolonged hydrolysis time (Butterworth, Warren, & Ellis, 2011).

2.3.2 First-order kinetics

When starch or starch-containing foods are digested *in vitro* with amylase or in combination with amyloglucosidase, the rate of reaction decreases as the time is extended and plots of the concentration of product formed (or quantity of starch digested) against time are logarithmic. The decrease of the digestion rate over time course is a natural feature of an exponential reaction (Butterworth, Warren, Grassby, Patel, & Ellis, 2012).This substrate decay process fits a single rate

coefficient (i.e., first-order equation) as follows (Goni, Garcia-Alonso, & Saura-Calixto, 1997).

$$C_t = C_\infty \left(1 - e^{-kt}\right)$$

where t is the digestion time (min), C_t is digested starch at incubation time t, C_∞ is digestion at infinite time, and k is rate constant (min^{-1}). One obvious problem in using this simple equation comes from the need for an accurate estimate of C_∞ (Butterworth, et al., 2012). Unless the enzyme-catalyzed digestion is allowed to run for a long time, digestibility curves cannot be guaranteed to have reached a true end point. In order to solve this problem, Butterworth, et al. (2012) introduced a modified Guggenheim method to calculate the rate constant where C_∞ is unknown, and the equation is cast in the form:

$$\ln\left(\frac{dC}{dt}\right) = \ln(C_\infty k) - kt$$

Thus, a plot of ln(dC/dt) against t is linear with a slope of $-k$, and the C_∞ can be calculated back from the intercept of the equation and slope k. The rate constant is a function of the fixed amylase and starch concentrations used in the digestion, and is therefore pseudo-first order. In addition, the physical structure of starches also plays an important role in determining the rate constant of starch digestion (B. Zhang, et al., 2013).

Figure 1 shows amylase digestion data and fitting plots of raw and cooked wheat and pea starches (Butterworth, et al., 2012). For the cooked wheat and pea starches, the whole digestion process can be well fitted by first-order behavior with a single rate constant (k value) under a porcine pancreatic amylase concentration of 0.165 IU/mL (2.25 nM). In contrast, granular starch digestion shows a two-phase kinetic profile at a higher amylase concentration of 0.33 IU/mL (4.5 nM). This suggests that there is a rapid digestion process that takes place in the first 20 min, likely due to hydrolysis of more available polymers attached to the surface of starch granules. The subsequent first-order rate process is believed to be the main single rate process with lower k value of the pea starch for both processes at an amylase concentration of 0.33 IU/mL (4.5nM) (Figure 1 C, D). Thus, the starch substrates do

not seem to consist of distinct structural fractions such as rapidly digestible and slowly digestible starches that differ in digestion rate. Instead, the amount of starch digested fraction in a given sample is under kinetic more than thermodynamic control (Htoon, et al., 2009; B. Zhang, et al., 2013), so starch fractions described as enzyme-resistant by remaining after digestion using a certain enzyme activity/time/temperature treatment can be further digested by e.g. application of more enzyme (Htoon et al, 2009). The first order model, however, cannot be directly applied in some *in vitro* cases, such as (i) those which use low catalytic dosages (giving a linear kinetic profile and resulting in zero-order kinetics (Warren, Zhang, Waltzer, Gidley, & Dhital, 2014), (ii) when inhibitory products are allowed to build up (Warren, Butterworth, & Ellis, 2012), and (iii) where structural and molecular changes take place during the digestion process such as in high-amylose maize starch (Htoon, et al., 2009; Lopez-Rubio, Flanagan, Shrestha, Gidley, & Gilbert, 2008).

[Insert Figure 1]

3 ERS from densely packed matrices: mechanisms and categories

As illustrated above, if starch chains are arranged in an appropriate form with high local molecular density, lower digestion rate/extent can be achieved with potential for human health benefit. This can occur either through reductions in the ability of amylase to bind to the substrate and/or reduction in the rate of enzyme action once bound. Two potential ways to produce densely packed ERS are (re-)crystallization and dense amorphous packing, which are reviewed below.

3.1 (Re-)crystallization

Retrogradation

Raw starches contain between 15% and 45% of crystalline material (Zobel, 1988a). The branch chains of amylopectin form double helices and contribute to starch crystallinity, whereas amylose is

291 considered to be in a largely amorphous state. The double helix packing arrangement and inter-
292 crystalline water of different types of starches might also differ, which can be identified by X-ray
293 diffraction or solid state ^{13}C NMR (Cheetham & Tao, 1998). The dense A-type crystal form of
294 starches is monoclinic with 8 water molecules per unit cell, whereas the B-type has a hexagonal unit
295 cell with 36 water molecules per unit cell, and is more open compared to monoclinic unit cells
296 (Imberty, Buleon, Tran, & Perez, 1991; Zobel, 1988b). These crystalline unit cells are disrupted
297 during cooking of starch in excess water, with a change from semi-crystalline starch structure to
298 amorphous conformation. However, during cooling and/or storage, gelatinized starch is transformed
299 from initially an amorphous state to a more ordered or crystalline state in a process termed
300 retrogradation.
301
302 The typical conformational changes of amylose during retrogradation are shown in Figure 2.
303 Amylose in aqueous solution exists as a random coil (Ring, I'Anson, & Morris, 1985) that can re-
304 crystallize into either A- or B-type double helices during cooling and the aging process of starch
305 dispersions, as a spontaneous process resulting in a metastable state of lower free energy (Gidley,
306 1989). Infinite aggregation of double helices generates a three-dimentional network with different
307 microstructure features such as cristallinity and porosity, which is based on interchain junction zones
308 of double helices with DP 10 – 100 (Gidley, et al., 1995). Retrograded amylose is thermally very
309 stable with a high melting temperature (120 - 170 ^{o}C), and amylose content and ERS yield are
310 normally positively correlated (Berry, 1986; Eerlingen & Delcour, 1995). Amylose re-crystallizes
311 much faster (completed within 24 h) than amylopectin (can continue for weeks) because of the linear
312 glucan structure and higher mobility of amylose (Eerlingen, Deceuninck, & Delcour, 1993;
313 Eerlingen, Jacobs, & Delcour, 1994). The branched nature of amylopectin inhibits its
314 recrystallization to some extent, and the partially crystallized amylopectin tends to form a network in
315 excess water (Fredriksson, Silverio, Andersson, Eliasson, & Aman, 1998; Miles, Morris, Orford, &

316 Ring, 1985). A low melting temperature in the range of 40 - 60 ^{o}C can be obseved, due to the
317 dimensions of the chains involved in the crystallisation process (Leeman, Karlsson, Eliasson, &
318 Bjorck, 2006). However, once debranched by isoamylase or pullulanase, the resulting short linear
319 chains become mobile and can retrograde as linear amylose chains. These retrograded chains were
320 shown to be effective in generating ERS (Cai & Shi, 2010).
321
322 [Insert Figure 2]
323
324 Storage time and temperature are critical factors in the formation of retrograded starch in an excess
325 of water and hence, a determinant of the rate of starch digestion. Thus, manipulation of starch
326 crystallization conditions is widely applied to control the digestibility of starch-based foods.
327 Eerlingen, Crombez, and Delcour (1993) found that ERS yields of retrograded wheat starch strongly
328 depend on the storage temperature and time, as shown in Figure 3. They found that initially (~15 min)
329 formation of ERS is favored at 0 ^{o}C (yield about 4%), whereas the ERS content (~10%) after
330 prolonged incubation was higher at 100 ^{o}C. The level of ERS at 68 ^{o}C had an intermediate formation
331 rate at either initial or extended stages. The initial fast formation of ERS was explained by
332 nucleation rate increases with decreasing temperature below the melting temperature (T_m, ~ 150 ^{o}C)
333 and above the glass transition temperature (T_g, ~ -5 ^{o}C). However, over a longer time period, crystal
334 growth was favored at 100 ^{o}C, closer to the T_m of the crystals. The theoretical maximum value of
335 crystallization rate (both nucleation and growth) is expected at a temperature T ≈ 1/2 (T_g + T_m),
336 which is close to 68 ^{o}C (Slade & Levine, 1987), whereas the real aggregation rate is faster at lower
337 temperatures due to decreased chain mobility (Gidley & Bulpin, 1989). A more effective way to
338 increase crystallization is to temperature cycle between low nucleation temperatures and high crystal
339 growth temperatures (Slade & Levine, 1987). It should be noted that ERS content did not increase
340 remarkably after reaching a plateau (Figure 3B), although the crystallinity increased with storage

time at higher temperatures (68 and 100 ^{o}C). The storage temperature also influenced the type of crystal: a B-type crystal formed at 0 and 68 ^{o}C, whereas A-type polymorph structure formed at 100 ^{o}C. The A-type polymorph is suggested to be a thermodynamic product with dense crystals, whereas the B-type polymorph is the kinetic product requiring the least entropy change from solution (Gidley, 1987). The B-type crystallites may form temporarily, but this structure may rearrange to form the more stable A-type structure. A general rule is that A-type crystallites are favored at high temperatures, short average chains, higher concentrations, and presence of salts, water-soluble alcohols, organic acids (Gidley, 1987; Montesanti, et al., 2010).

[Insert Figure 3]

Gidley and Bulpin (1989) found that re-crystallization and gelation behavior of amylose in aqueous solution (0.2 – 5.0 %) show a dependence on chain length (synthesized *in vitro* using potato phosphorylase, degree of polymerization (DP) ranging from 40 to 2800). The maximum re-crystallization rate was found for chain lengths of ~ 100 residues in dilute (< 0.1 %) solution at initial stages of the process, corresponding to the so-called “dissolving gap” for amylose in the DP range 35-900 (Burchard, 1963). Short-chain amylose (DP < 110) can be re-crystallized at all concentration up to 5.0 % upon cooling hot aqueous solution (70 – 80 ^{o}C). More specifically, amylose with DP 40 and 65 results in fine and dense re-crystallized precipitates, whereas precipitates from DP 90 and 110 are less dense. For the amylose with DP from 250 to 600, both re-crystallization and gelation occur for chain lengths of 250-660 residues, depending on the amylose concentration. For long-chain amylose (DP > 1100), gelation predominates over re-crystallization at all concentrations, due to the formation of a macromolecular network with extensive cross-linking (via hydrogen bonding and/or hydrophobic interactions). Eerlingen, Deceuninck, et al. (1993) found that the chain length (DP 19 - 26) and crystalline structure (type and crystallinity level) of the ERS obtained is independent to the

amylose chain length (DP 40 - 610). A minimum DP of 10 and a maximum of 100 seems to be necessary to form the double helix (Gidley, et al., 1995). However, according to Eerlingen, Deceuninck, et al. (1993), the yield of ERS increased with DP (~19 %, DP 40) to plateau values of 23 – 28 % (DP 100 - 610). It was postulated that short-chain amylose (DP 40 - 100) contains a relatively high concentration of chains that do not have dimensions critical for incorporation in the crystalline structure.

Although it is well understood that the molecular basis for amylose aggregation is the adoption of a left-handed, parallel-stranded double helical conformation followed by helix-helix aggregation (Gidley, 1989), mesoscopic information on retrograded starch is limited, particularly for the amorphous fraction. The amorphous fraction can be more easily degraded by acid than the crystalline fraction. It was proposed to consist of dangling chains ($6 < DP < 30$) and linked to double helices in the macroporous network, and proposed to be mainly responsible for the hydrodynamic behavior and the network porosity (Leloup, Colonna, Ring, Roberts, & Wells, 1992). Cairns, Sun, Morris, and Ring (1995) prepared retrograded amylose gels and studied their ERS fraction after 24 h enzyme hydrolysis at 37 ^{o}C. The storage time (1 or 7 day) and enzyme hydrolysis did not affect the average molecular weight (DP 66) and size (8.3 nm) of retrograded crystallites, although the crystallinity of amylose gels with 7 days of storage was ca. 2 times higher than that of 1 day storage. They found that the ERS yield non-linearly increased with the level of crystallinity, due to a slow formation of perfect crystals from some internal defects. One model that was postulated is that the crystals (~10 nm long) may be discontinuous, with a substantial amorphous portion shielded from enzyme digestion by entrapment within the crystal structure (Cairns, et al., 1995; J. L. Jane & Robyt, 1984). In principle, if starch polymers are arranged in a dense enough form (i.e., high local molecular density), they can decrease the digestion rate even if the food matrices are amorphous. G. Y. Zhang, Ao, and Hamaker (2006) reported that the crystalline and amorphous contents of partially digested

391 granular starches were unchanged from the native values. This could either mean that (as suggested
392 by the authors) both crystalline and amorphous regions are digested side-by-side, suggesting that
393 local density of non-order structures formed by plant biosynthesis is as high as that of crystalline
394 regions, or that the rate-limiting step for enzymic hydrolysis of granules occurs prior to active
395 digestion i.e. binding is rate-limiting and any differences between the intrinsic rate of digestion of
396 crystalline and amorphous fractions are small compared to a slower binding step (Dhital, Warren,
397 Butterworth, et al., 2014). In either case, non-crystalline material apparently contributes to the rate-
398 limiting step, again illustrating the concept that it is not only crystalline material that can achieve
399 sufficiently high molecular density to slow down amylase digestion.
400
401 It should be emphasised that the ERS is a measurement- and method-oriented concept, i.e., the
402 enzyme resistance is explained by the limited time and concentration that the enzymes act on the
403 starch substrate. Bird, Lopez-Rubio, Shrestha, and Gidley (2009) suggested that the ERS yield of
404 retrograded starch depends on the competition between the retrogradation kinetics (influencing local
405 density of starch chains) and the kinetics of enzyme digestion. It seems likely that crystallization is
406 only one route to achieving a dense packing of starch chains which hinders the enzyme accessibility
407 or catalytic action, and dense packing of non-crystalline starch polymers may also be an effective
408 mechanism for slowing digestion.
409
410 Amylose-lipid complex
411 Complexes between amylose and lipids, such as monoglycerides, fatty acids, lysophospholipids and
412 surfactants, can significantly reduce the digestion rate and extent both *in vitro* and *in vivo*,
413 representing another source of resistant starch (Ai, et al., 2013; Hasjim, et al., 2010). Amylopectin
414 probably binds only one lipid per individual chain, and the complex formation retards the
415 retrogradation process (A. C. Eliasson & Ljunger, 1988; B. Zhang, et al., 2012). Two distinct forms

of amylose-lipid complexes have been defined based on the transition peak temperature: an amorphous form (Form I) that melts at a lower temperature (T_p < 100 ^oC) in differential scanning calorimetry thermograms, and a crystalline form (Form II) that has the V-type crystalline structure with a characteristic X-ray diffraction pattern with peaks around 7.5^o, 13^{o}and 20^o (2θ) and a higher melting temperature (T_p, 115 - 125 ^oC) (Tufvesson, Wahlgren, & Eliasson, 2003a, 2003b). Form I appears to have randomly oriented helices, whereas Form II has an ordered organization of amylose complexes. The amorphous form is less rigid and stable, and can be converted to the crystalline form through annealing at a temperature above the melting temperature of Form I but lower than that of Form II. Both the lipid/starch used and incubation conditions affect the complex formation: a general rule is that crystalline form are favored at higher temperatures, longer incubation time, longer amylose chain lengths, longer chain lengths of saturated lipids, lower unsaturation degree of lipids, lower number of *cis*- double bonds in the complexing lipid, as summarized by A.-C. Eliasson and Wahlgren (2004). Ionic head groups of lipids and chemically modified starch will not favor the formation of ordered type II structures (Kowblansky, 1985).

Godet, Bouchet, Colonna, Gallant, and Buleon (1996) proposed a two-stage formation mechanism of the crystalline amylose-lipid complexes (Form II): (1) the formation of amylose-lipid complexes, in which each amylose chain is complexed with one or more lipid molecules and (2) the aggregation of complexes in a fringed micellar arrangement or a U-shaped folding. The crystalline complexes have helical chain segments ordered in structures with dimensions up to 14.5 nm (Galloway, Biliaderis, & Stanley, 1989). The densely packed crystallized amylose-lipid complexes are supposed to be resistant to digestive enzymes. The enzymatic susceptibility of amylose has been ranked in the following way by Tufveson et al (2001): amorphous amylose > amylose-lipid complex > retrograded amylose (Tufvesson, Skrabanja, Björck, Elmståhl, & Eliasson, 2001). Seneviratne and Biliaderis (1991) found that the crystallinity level of the complex matrices was inversely related to the

digestion rate and extent. However, this is not always the case as Tufvesson, et al. (2001) reported that there was no difference in digestibility between amorphous Form I and crystalline Form II complex. It is therefore likely that it is the amylose-lipid complex that is important for enzyme digestion resistance rather than crystallization. The concept that single helices of complexed molecules are oriented perpendicular to the plane of the lamellae has been agreed (Buleon, Duprat, Booy, & Chanzy, 1984; J. L. Jane & Robyt, 1984). However, what the differences are between how the amorphous and crystalline forms are organized which further affects the local molecular density of the complex matrices, is not clear. We suggest that the nature of enzyme resistance of complex matrices has its origin in local chain density at the nanometer length scale which is relevant to binding/catalysis by amylase, rather than an average value of crystallinity.

Hydrothermal treatment

Annealing and heat-moisture treatment are two hydrothermal treatments that modify starch properties such as digestibility. Both processes involve incubation of starches in excess (> 60%) or intermediate (40 – 55%) water (annealing) or at low (< 35%) moisture levels (heat-moisture treatment) for a certain period of time, at a mobile rubbery state with a temperature above the glass transition temperature but below the gelatinization temperature (Jacobs & Delcour, 1998). Heat-moisture treatment is carried out at higher temperatures (90 - 120 ^{o}C), while annealing occurs below the gelatinization temperature of starches. Annealing does not change the overall repeat distance of crystalline and amorphous lamellae (Jacobs & Delcour, 1998; Jacobs, et al., 1998), but allows individual molecular reorganization and improves the crystalline perfection between starch chains (Tester & Debon, 2000). The crystallinity level (judged by X-ray diffraction) and interactions between starch chains in the amorphous and crystalline regions are increased after annealing treatment (Lan, et al., 2008), which may be expected to affect the digestion properties. A slight decrease in enzyme susceptibility after annealing was found for wheat, lentil, high-amylose maize

and potato starches, presumably due to increased crystallite perfection and enhanced amylose–amylose and/or amylose–amylopectin interactions (Brumovsky & Thompson, 2001; Hoover & Vasanthan, 1993). We note that the enhanced ordering of double helices and improved alignments of starch chains is a route to achieve higher local density of helical structure through annealing. However, it was found that the impact of annealing on enzyme susceptibility can depend on starch botanical origin. Annealed barley, oat and sago starches are more easily hydrolyzed by α-amylases than native starches (Hoover & Vasanthan, 1993; Lauro, Suortti, Autio, Linko, & Poutanen, 1993). Although the molecular reorganization of starch is slightly improved during annealing, the original starch architectures such as granule size, surface features may be more important with respect to digestion pattern/rate/extent in some cases.

Heat-moisture treatment under higher temperatures and low moisture promotes disruption of the crystalline structure and dissociation of the double helical structure in the amorphous region, followed by the rearrangement of the disrupted crystals (Gunaratne & Hoover, 2002). The extent of these structural changes normally depends on botanical origin, accompanying changes to crystalline pattern (B to A + B) and level, physicochemical and digestion properties. Tuber or root starches are more sensitive to heat-moisture treatment than legume or cereal starches (Zavareze & Dias, 2011). Normally, an increased digestibility of starch granules has been shown to occur following heat-moisture treatment, depending on treatment conditions and quantitatively varying among starch sources. In the case of potato and yam starches, crystalline disruption near the granule surface can degrade the outer physical barrier of these starch granules, decreasing the local molecular density of starch chains, consequently facilitating enzyme access and binding to starch granules (Gunaratne & Hoover, 2002). Furthermore, the decreased digestibility also could result from the disruption of the double helices within the granules.

Although there are relationships between re-crystallization and densification of starch matrices, which would be expected to impact the enzymatic susceptibility (Dhital, Warren, Butterworth, et al., 2014), it seems that crystallization is probably not only one route to achieving a dense packing of starch chains. This suggests that locally-dense non-crystalline structures could also decrease/prevent accessibility or action of enzymes. The factors affecting the formation of amorphous matrices may also impact on re-crystallization processes, although this is less studied and understood up to now.

3.2 Non-crystalline dense packing

Although it is generally accepted that crystalline type and level of crystallinity must play some role in determining digestion rate and extent of starches, recent reports have shown that crystallinity may not be directly linked with the percentage of ERS obtained (Htoon, et al., 2009; Lopez-Rubio, Htoon, & Gilbert, 2007). Even for native starches, crystallinity alone also cannot explain the resistance to digestion. For example, the limited digestion rate of B-type polymorphic starches is controlled by surface barriers more than crystallinity (Dhital, et al., 2010). On the other hand, some almost amorphous starch materials provide high levels of the resistant fraction (Chanvrier, et al., 2007; Htoon, et al., 2009). Thus, although crystallinity is one way to achieve local molecular density, it appears that non-crystalline chains can also pack in an enzyme-resistant form that is currently poorly understood and brings a new research challenge for food/polymer chemists.

Amorphous (also called ‘non-crystalline’) state is essentially a negative definition based on the absence of detectable molecular order, therefore making it difficult to quantify the molecular conformation of the matrices. From the evidence presented above, the measurement of local molecular density of starch matrices is the key to understanding the fundamental mechanism(s) of ERS from non-crystalline dense packing. However, the current technical ability to measure sub-micron variability of local density in starch/food matrices remains limited. From the current data

516 available, non-crystalline starch with lower digestion rate and extent can be achieved by either (1)
517 dense molecular structures at nanometer length scale or (2) densely packed matrices at
518 (sub)micrometer length scale.
519
520 Dense molecular structures
521 Although the dense molecular structures leading to ERS character are often found in retrograded
522 starch and starch-lipid complex as an aggregated/crystallized form, the double/single helices not
523 involved in crystallites also can render the α-1,4 glucosidic linkages inaccessible to starch degrading
524 enzymes. A- and B-type single crystals exhibit a 6-fold, left-handed double helical conformation
525 with repeat distances of 2.13 and 2.08 nm respectively (Hsein-Chih & Sarko, 1978; Hsien-Chih &
526 Sarko, 1978; Imberty & Perez, 1988). Aside from the differences in the amount of water discussed
527 previously, the A- and B- type crystals differ only in that the former has a denser packed-structure,
528 whereas the latter is more open. In aqueous solution at room temperature, starch chains with DP <
529 10 do not crystallize, while the A-type crystals resulted from starch chains with DP from 10 to 12;
530 chains longer than 12 crystallize as B-type (Pfannemüller, 1987). The crystalline type can also be
531 affected by crystallization at various water/alcohol concentrations, for example, A-, B- and V-type
532 polymorph single crystals are precipitated at 15%, 0%, and 40% of ethanol concentration
533 respectively (Buleon, et al., 1984).
534
535 In a recent study, we found that there is a small fraction of single crystals (2 - 4 %, calculated by
536 weight) present in starch granule 'ghosts' (the insoluble remnant after low shear cooking of
537 starches), and which could be enzyme resistant (B. Zhang, Dhital, et al., 2014). The single crystals
538 can be either V-type order based on amylose (for maize ghosts) or B-type order from amylopectin for
539 potato ghosts. From investigation of molecular components and glucan conformation for ghosts and
540 ghost remnants after enzyme hydrolysis, we found that starch ghosts are enriched in amylopectin

541 within ghost remnants (B. Zhang, Dhital, et al., 2014). Therefore, we concluded that the ghost
542 structure originates primarily from physical entanglements of highly-branched and large molecular
543 size amylopectin molecules. This not only confirms that double helices or crystallites are not
544 necessary to strengthen ghost structure but also illustrates the possibility of achieving enzyme
545 resistance from essentially amorphous (96 - 98%) matrices.
546
547 Densely packed matrices
548 Generally, starch supramolecular and granular structures are disrupted by thermal, moisture and
549 energy inputs during extrusion cooking, which would be expected to increase the accessibility of
550 starch-acting enzymes to starch polymers. However, among extrudates from different starch species,
551 high-amylose maize starch after extrusion and storage shows a relatively high yield of ERS (>20%)
552 (Chanvrier, et al., 2007). A number of extrusion parameters such as feed moisture, temperature,
553 screw speed and storage conditions are known to affect the ERS content of extrudates. Extrusion of
554 starch in the presence of sufficient water triggers a number of physicochemical and functionality
555 changes in starch granules, such as the loss of granular structure associated with melting of
556 crystallites and underlying helices, and generating an amorphous structure (Bird, et al., 2009; Faraj,
557 Vasanthan, & Hoover, 2004). This would be expected to increase the vulnerability of starch to
558 amylase digestion. Upon cooling, hydrated amylose (and amylopectin) chains may undergo
559 retrogradation by molecular re-association into double helices, and may consequently acquire
560 resistance to enzyme digestion (Htoon, et al., 2009). Therefore, extruded products may also lead to a
561 higher RS content. Htoon, et al. (2009) reported that almost amorphous extrudate (~5% crystallinity)
562 from high-amylose maize starch could deliver high ERS contents (~20%) *in vitro*, and that more
563 generally there was no apparent correlation between ERS and crystallinity level from X-ray
564 diffraction (Figure 4). The presence of amorphous material in the enzyme-resistant fractions is also
565 consistent with resistance based on a kinetic mechanism rather than a specific crystalline structure

566 that is completely undigested (Lopez-Rubio, et al., 2008). Shrestha, et al. (2010) suggested that
567 enzyme-resistance might be associated with a dense solid phase structure that is even non-/weakly-
568 crystalline. X-ray scattering studies showed that the preferred characteristic dimension of the crystals
569 formed was ~5 nm, suggesting that resistant crystals could be formed from chains with a maximum
570 DP of ~13 and ~17 glucose units for double and single helices respectively with potential
571 amorphous fringed ends (Lopez-Rubio, et al., 2008). We suggest that the local density of packing of
572 starch chains controls its digestibility rather than just crystallinity, which represents just one
573 mechanism of achieving high chain density. If these molecularly dense structures are aligned rigidly
574 they could resist digestion and become ERS with health benefits.
575
576 Amorphous amylose-lipid complex (Form I) is another good example of non-crystalline ERS from
577 densely packed matrices. Although the structure without obvious X-ray diffraction peaks is less rigid
578 and thermo-stable, Tufvesson, et al. (2001) found that there was no difference in digestibility
579 between amorphous Form I and crystalline Form II complex under the preparation conditions used.
580 That suggests that amorphous matrices can escape digestion under certain enzyme concentrations if
581 the starch polymers are densely enough packed, which can be an effective mechanism for slow
582 digestion rate/extent.
583
584 Other potential methods to achieve high ERS yields from largely amorphous granular starches
585 include freeze-drying, dense protein network formation et al. Recently, we reported that the
586 crystallinity and molecular order of B-type polymorphic starches can be greatly degraded (e.g.,
587 potato starch lost ~50% crystallinity and ~40% double helical order) by freeze-drying, possibly due
588 to higher amount of intracrystalline water or longer branch chains in B-type starches (B. Zhang,
589 Wang, et al., 2014). The dense protein network formed in pasta can also limit the access and binding

590 of enzyme to embedded starch granules, and restrict the diffusion of water to the granules that
591 reduces the starch gelatinisation to some extent (Colonna, et al., 1990).

592

593 Apart from processed starchy food, non-crystalline dense packing also exists in nature. The
594 amorphous growth rings within starch granules are perhaps the best representative. In contrast to
595 semi-crystalline layers consisting of amylopectin clusters that in turn contain alternating crystalline
596 and amorphous lamellae, amorphous growth rings are thought to contain amylose and amylopectin
597 molecules in apparently unordered conformation. The number and thickness of amorphous layers
598 depends on the botanical origin and amylose content (Yuryev, et al., 2004). According to Cameron
599 and Donald (1992), the amorphous growth ring is at least as thick as the semi-crystalline one, which
600 is thought to be 120~500 nm (Cameron & Donald, 1992). As discussed previously, G. Y. Zhang, et
601 al. (2006) reported that the crystalline and amorphous growth rings of granular starches are
602 apparently digested side-by-side, suggesting local density of amorphous growth rings is enough high
603 to limit enzyme binding therefore achieve similar digestion rates as crystalline materials.

604

605 [Insert Figure 4]

606

607 **4 Concluding remarks and future directions**

608 Understanding the fundamental mechanism of ERS from dense matrices either by recrystallization or
609 non-crystalline packing is useful for designing the next-generation of starch-containing foods to be
610 more available to consumers/industry in response to many diet-related diseases including type II
611 diabetes and obesity. This review summarized the role of local molecular density on starch digestion
612 kinetics, with the emphasis being that density sufficient to either prevent/limit binding and/or slow
613 down catalysis can be achieved by either re-crystallization or dense amorphous packing. The M-M
614 and first order kinetics and data interpretation commonly used for *in vitro* starch digestion were also

615 briefly discussed. Whilst considerable progress has been made, further studies will need to be
616 conducted, including
617 1. Amorphous state is essentially a negative definition based on the absence of detectable molecular
618 order. Further work is required to better understand the nature of non-crystalline matrices that result
619 in slow digestion rate/extent, such as the local density and entanglement of starch chains through
620 application of material and polymer science principles.
621 2. Methods such as positron annihilation lifetime spectroscopy may provide improved methods for
622 determining local molecular densities of starch matrices in a non-destructive manner (Liao, et al.,
623 2011; Liu, et al., 2012). This will be a key challenge in fundamental starch research.
624 3. Methods to increase the molecular densities of starch matrices independent of crystallinity should
625 be developed. This will provide practical outcomes including better methods for increasing RS in
626 processed starches. It will also be a significant advance in starch theory, and the understanding of
627 non-crystalline dense packing.
628 4.
629 Determine what aspects of high-amylose starches contribute to their relative susceptibility to dense
630 packing during extrusion. This will advance our theoretical understanding of the physical packing of
631 amylose in amorphous matrices, importantly within granules.
632

633 **Acknowledgements**

634 This work was supported by the Australian Research Council Centre of Excellence in Plant Cell
635 Walls.
636

637 **References**

638 Abdullah, M., French, D., & Robyt, J. F. (1966). Multiple attack by alpha-amylases. *Archives of*
639 *Biochemistry and Biophysics, 114*, 595-563.

640 Ai, Y. F., Hasjim, J., & Jane, J. L. (2013). Effects of lipids on enzymatic hydrolysis and physical
641 properties of starch. *Carbohydrate Polymers, 92*, 120-127.
642 Al-Rabadi, G. J., Torley, P. J., Williams, B. A., Bryden, W. L., & Gidley, M. J. (2011). Effect of
643 extrusion temperature and pre-extrusion particle size on starch digestion kinetics in barley
644 and sorghum grain extrudates. *Animal Feed Science and Technology, 168*, 267-279.
645 Andersson, H. (1992). The ileostomy model for the study of carbohydrate digestion and carbohydrate
646 effects on sterol excretion in man. *European Journal of Clinical Nutrition, 46*, S69-S76.
647 Ao, Z., Simsek, S., Zhang, G., Venkatachalam, M., Reuhs, B. L., & Hamaker, B. R. (2007). Starch
648 with a slow digestion property produced by altering its chain length, branch density, and
649 crystalline structure. *Journal of Agricultural and Food Chemistry, 55*, 4540-4547.
650 Bai, Y. J., Cai, L. M., Doutch, J., Gilbert, E. P., & Shi, Y. C. (2014). Structural changes from native
651 waxy maize starch granules to cold-water-soluble pyrodextrin during thermal treatment.
652 *Journal of Agricultural and Food Chemistry, 62*, 4186-4194.
653 Behall, K. M., & Hallfrisch, J. (2002). Plasma glucose and insulin reduction after consumption of
654 breads varying in amylose content. *European Journal of Clinical Nutrition, 56*, 913-920.
655 Berry, C. S. (1986). Resistant starch - Formation and measurement of starch that survives exhaustive
656 digestion with amylolytic enzymes during the determination of dietary fiber. *Journal of*
657 *Cereal Science, 4*, 301-314.
658 Bird, A. R., Lopez-Rubio, A., Shrestha, A. K., & Gidley, M. J. (2009). Resistant starch in vitro and
659 in vivo: Factors determining yield, structure, and physiological relevance. In S. Kasapis,
660 Norton, I. T., & Ubbink, J. B. (Ed.), *Modern Biopolymer Sciences* (pp. 449–510). London:
661 Academic Press.
662 Brand-Miller, J. C., Holt, S. H. A., Pawlak, D. B., & McMillan, J. (2002). Glycemic index and
663 obesity. *American Journal of Clinical Nutrition, 76*, 281S-285S.
664 Brumovsky, J. O., & Thompson, D. B. (2001). Production of boiling-stable granular resistant starch
665 by partial acid hydrolysis and hydrothermal treatments of high-amylose maize starch. *Cereal*
666 *Chemistry, 78*, 680-689.
667 Buisson, G., Duee, E., Haser, R., & Payan, F. (1987). Three dimensional structure of porcine
668 pancreatic alpha-amylase at 2.9 a resolution. Role of calcium in structure and activity. *Embo*
669 *Journal, 6*, 3909-3916.
670 Buleon, A., Duprat, F., Booy, F. P., & Chanzy, H. (1984). Single-crystals of amylose with a low
671 degree of polymerization. *Carbohydrate Polymers, 4*, 161-173.
672 Burchard, W (1963). Das viskositätsverhalten von amylose in verschiedenen lösungsmitteln.
673 *Makromol. Chem. 64*,110-125.

Butterworth, P. J., Warren, F. J., & Ellis, P. R. (2011). Human alpha-amylase and starch digestion: An interesting marriage. *Starch/Starke, 63*, 395-405.

Butterworth, P. J., Warren, F. J., Grassby, T., Patel, H., & Ellis, P. R. (2012). Analysis of starch amylolysis using plots for first-order kinetics. *Carbohydrate Polymers, 87*, 2189-2197.

Cai, L., & Shi, Y.-C. (2010). Structure and digestibility of crystalline short-chain amylose from debranched waxy wheat, waxy maize, and waxy potato starches. *Carbohydrate Polymers, 79*, 1117-1123.

Cairns, P., Sun, L., Morris, V. J., & Ring, S. G. (1995). Physicochemical studies using amylose as an in vitro model for resistant starch. *Journal of Cereal Science, 21*, 37-47.

Cameron, R. E., & Donald, A. M. (1992). A small-angle X-ray scattering study of the annealing and gelatinization of starch. *Polymer, 33*, 2628-2636.

Champ, M. M. J. (2004). Physiological aspects of resistant starch and in vivo measurements. *Journal of Aoac International, 87*, 749-755.

Chanvrier, H., Uthayakumaran, S., Appelqvist, I. A. M., Gidley, M. J., Gilbert, E. P., & Lopez-Rubio, A. (2007). Influence of storage conditions on the structure, thermal behavior, and formation of enzyme-resistant starch in extruded starches. *Journal of Agricultural and Food Chemistry, 55*, 9883-9890.

Cheetham, N. W. H., & Tao, L. P. (1998). Variation in crystalline type with amylose content in maize starch granules: an X-ray powder diffraction study. *Carbohydrate Polymers, 36*, 277-284.

Colonna, P., Barry, J. L., Cloarec, D., Bornet, F., Gouilloud, S., & Galmiche, J. P. (1990). Enzymic susceptibility of starch from pasta. *Journal of Cereal Science, 11*, 59-70.

Colonna, P., Leloup, V., & Buleon, A. (1992). Limiting factors of starch hydrolysis. *European Journal of Clinical Nutrition, 46*, S17-S32.

Cooke, D., & Gidley, M. J. (1992). Loss of crystalline and molecular order during starch gelatinization: Origin of the enthalpic transition. *Carbohydrate Research, 227*, 103-112.

Dhital, S., Lin, A. H. M., Hamaker, B. R., Gidley, M. J., & Muniandy, A. (2013). Mammalian mucosal alpha-glucosidases coordinate with alpha-amylase in the initial starch hydrolysis stage to have a role in starch digestion beyond glucogenesis. *PLoS ONE, 8*, e62546.

Dhital, S., Shrestha, A. K., & Gidley, M. J. (2010). Relationship between granule size and in vitro digestibility of maize and potato starches. *Carbohydrate Polymers, 82*, 480-488.

Dhital, S., Warren, F. J., Butterworth, P. J., Ellis, P. R., & Gidley, M. J. (2014). Mechanisms of starch digestion by alpha-amylase: Structural basis for kinetic properties. *Critical Reviews in Food Science and Nutrition*, Accepted for publication

Dhital, S., Warren, F. J., Zhang, B., & Gidley, M. J. (2014). Amylase binding to starch granules under hydrolysing and non-hydrolysing conditions. *Carbohydrate Polymers, 113*, 97-107.

Eerlingen, R. C., Crombez, M., & Delcour, J. A. (1993). Enzyme-resistant starch .1. Quantitative and qualitative influence of incubation-time and temperature of autoclaved starch on resistant starch formation. *Cereal Chemistry, 70*, 339-344.

Eerlingen, R. C., Deceuninck, M., & Delcour, J. A. (1993). Enzyme-resistant starch .2. Influence of amylose chain-length on resistant starch formation. *Cereal Chemistry, 70*, 345-350.

Eerlingen, R. C., & Delcour, J. A. (1995). Formation, analysis, structure and properties of type-III enzyme resistant starch. *Journal of Cereal Science, 22*, 129-138.

Eerlingen, R. C., Jacobs, H., & Delcour, J. A. (1994). Enzyme-resistant starch .5. Effect of retrogradation of waxy maize starch on enzyme susceptibility. *Cereal Chemistry, 71*, 351-355.

Eliasson, A.-C., & Wahlgren, M. (2004). Starch-lipid interactions and their relevance in food products. *Starch in food: structure, function, and applications. Woodhead, Cambridge*, 441-454.

Eliasson, A. C., & Ljunger, G. (1988). Interactions between Amylopectin and Lipid Additives during Retrogradation in a Model System. *Journal of the Science of Food and Agriculture, 44*, 353-361.

Englyst, H. N., & Cummings, J. H. (1985). Digestion of the Polysaccharides of Some Cereal Foods in the Human Small-Intestine. *American Journal of Clinical Nutrition, 42*, 778-787.

Englyst, H. N., Kingman, S. M., & Cummings, J. H. (1992). Classification and measurement of nutritionally important starch fractions. *European Journal of Clinical Nutrition, 46*, S33-S50.

Englyst, H. N., Kingman, S. M., Hudson, G. J., & Cummings, J. H. (1996). Measurement of resistant starch in vitro and in vivo. *British Journal of Nutrition, 75*, 749-755.

Englyst, H. N., & Macfarlane, G. T. (1986). Breakdown of resistant and readily digestible starch by human gut bacteria. *Journal of the Science of Food and Agriculture, 37*, 699-706.

Faraj, A., Vasanthan, T., & Hoover, R. (2004). The effect of extrusion cooking on resistant starch formation in waxy and regular barley flours. *Food Research International, 37*, 517-525.

Fredriksson, H., Silverio, J., Andersson, R., Eliasson, A. C., & Aman, P. (1998). The influence of amylose and amylopectin characteristics on gelatinization and retrogradation properties of different starches. *Carbohydrate Polymers, 35*, 119-134.

Fujii, M., Homma, T., & Taniguchi, M. (1988). Synergism of alpha-amylase and glucoamylase on hydrolysis of native starch granules. *Biotechnology and Bioengineering, 32*, 910-915.

741 Gallant, D. J., Bouchet, B., & Baldwin, P. M. (1997). Microscopy of starch: Evidence of a new level
742 of granule organization. *Carbohydrate Polymers, 32*, 177-191.
743 Galloway, G. I., Biliaderis, C. G., & Stanley, D. W. (1989). Properties and structure of amylose‐
744 glyceryl monostearate complexes formed in solution or on extrusion of wheat flour. *Journal*
745 *of Food Science, 54*, 950-957.
746 Gidley, M. J. (1987). Factors affecting the crystalline type (A-C) of native starches and model
747 compounds - A rationalisation of observed effects in terms of polymorphic structures.
748 *Carbohydrate Research, 161*, 301-304.
749 Gidley, M. J. (1989). Molecular mechanisms underlying amylose aggregation and gelation.
750 *Macromolecules, 22*, 351-358.
751 Gidley, M. J. (2013). Hydrocolloids in the digestive tract and related health implications. *Current*
752 *Opinion in Colloid & Interface Science, 18*, 371-378.
753 Gidley, M. J., & Bociek, S. M. (1985). Molecular organization in starches: A 13C CP/MAS NMR
754 study. *Journal of American Chemical Society, 107*, 7040-7044.
755 Gidley, M. J., & Bulpin, P. V. (1989). Aggregation of amylose in aqueous systems: The effect of
756 chain-length on phase-behavior and aggregation kinetics. *Macromolecules, 22*, 341-346.
757 Gidley, M. J., Cooke, D., Darke, A. H., Hoffmann, R. A., Russell, A. L., & Greenwell, P. (1995).
758 Molecular order and structure in enzyme-resistant retrograded starch. *Carbohydrate*
759 *Polymers, 28*, 23-31.
760 Gilles, C., Astier, J. P., MarchisMouren, G., Cambillau, C., & Payan, F. (1996). Crystal structure of
761 pig pancreatic alpha-amylase isoenzyme II, in complex with the carbohydrate inhibitor
762 acarbose. *European Journal of Biochemistry, 238*, 561-569.
763 Godet, M., Bouchet, B., Colonna, P., Gallant, D., & Buleon, A. (1996). Crystalline amylose‐fatty
764 acid complexes: Morphology and crystal thickness. *Journal of Food Science, 61*, 1196-1201.
765 Goni, I., Garcia-Alonso, A., & Saura-Calixto, F. (1997). A starch hydrolysis procedure to estimate
766 glycemic index. *Nutrition Research, 17*, 427-437.
767 Gunaratne, A., & Hoover, R. (2002). Effect of heat–moisture treatment on the structure and
768 physicochemical properties of tuber and root starches. *Carbohydrate Polymers, 49*, 425-437.
769 Hasjim, J., Lee, S.-O., Hendrich, S., Setiawan, S., Ai, Y., & Jane, J.-l. (2010). Characterization of a
770 novel resistant-starch and its effects on postprandial plasma-glucose and insulin responses.
771 *Cereal Chemistry, 87*, 257-262.
772 Hiromi, K., Nitta, Y., Numata, C., & Ono, S. (1973). Subsite affinities of glucoamylase: Examination
773 of validity of subsite theory. *Biochimica Et Biophysica Acta, 302*, 362-375.

774 Hizukuri, S. (2006). *Starch: Analytical aspects* (Vol. 74): CRC Press.
775 Holm, L., Koivula, A. K., Lehtovaara, P. M., Hemminki, A., & Knowles, J. K. C. (1990). Random
776 mutagenesis used to probe the structure and function of Bacillus-Stearothermophilus alpha-
777 amylase. *Protein Engineering, 3*, 181-191.
778 Hoover, R., & Vasanthan, T. (1993). The effect of annealing on the physicochemical properties of
779 wheat, oat, potato and lentil starches. *Journal of Food Biochemistry, 17*, 303-325.
780 Hsein-Chih, H. W., & Sarko, A. (1978). The double-helical molecular structure of crystalline B-
781 amylose. *Carbohydrate Research, 61*, 7-25.
782 Hsien-Chih, H. W., & Sarko, A. (1978). The double-helical molecular structure of crystalline A-
783 amylose. *Carbohydrate Research, 61*, 27-40.
784 Htoon, A., Shrestha, A. K., Flanagan, B. M., Lopez-Rubio, A., Bird, A. R., Gilbert, E. P., & Gidley,
785 M. J. (2009). Effects of processing high amylose maize starches under controlled conditions
786 on structural organisation and amylase digestibility. *Carbohydrate Polymers, 75*, 236-245.
787 Imberty, A., Buleon, A., Tran, V., & Perez, S. (1991). Recent advances in knowledge of starch
788 structure. *Starch/Starke, 43*, 375-384.
789 Imberty, A., & Perez, S. (1988). A revisit to the three‐dimensional structure of B‐type starch.
790 *Biopolymers, 27*, 1205-1221.
791 Jacobs, H., & Delcour, J. A. (1998). Hydrothermal modifications of granular starch, with retention of
792 the granular structure: A review. *Journal of Agricultural and Food Chemistry, 46*, 2895-
793 2905.
794 Jacobs, H., Mischenko, N., Koch, M. H., Eerlingen, R. C., Delcour, J. A., & Reynaers, H. (1998).
795 Evaluation of the impact of annealing on gelatinisation at intermediate water content of wheat
796 and potato starches: A differential scanning calorimetry and small angle X-ray scattering
797 study. *Carbohydrate Research, 306*, 1-10.
798 Jane, J.-L. (2006). Current understanding on starch granule structures. *Journal of Applied*
799 *Glycoscience, 53*, 205-213.
800 Jane, J.-L., Chen, Y. Y., Lee, L. F., McPherson, A. E., Wong, K. S., Radosavljevic, M., &
801 Kasemsuwan, T. (1999). Effects of amylopectin branch chain length and amylose content on
802 the gelatinization and pasting properties of starch. *Cereal Chemistry, 76*, 629-637.
803 Jane, J. L., & Robyt, J. F. (1984). Structure studies of amylose-V complexes and retrograded
804 amylose by acation of alpha-amylases, and a new method for preparing amylodextrins.
805 *Carbohydrate Research, 132*, 105-118.

806 Kandra, L., & Gyemant, G. (2000). Examination of the active sites of human salivary alpha-amylase
807 (HSA). *Carbohydrate Research, 329*, 579-585.
808 Kowblansky, M. (1985). Calorimetric investigation of inclusion complexes of amylose with long-
809 chain aliphatic compounds containing different functional groups. *Macromolecules, 18*,
810 1776-1779.
811 Lan, H., Hoover, R., Jayakody, L., Liu, Q., Donner, E., Baga, M., Asare, E., Hucl, P., & Chibbar, R.
812 (2008). Impact of annealing on the molecular structure and physicochemical properties of
813 normal, waxy and high amylose bread wheat starches. *Food Chemistry, 111*, 663-675.
814 Lauro, M., Suortti, T., Autio, K., Linko, P., & Poutanen, K. (1993). Accessibility of barley starch
815 granules to alpha-amylase during different phases of gelatinization. *Journal of Cereal*
816 *Science, 17*, 125-136.
817 Le Corre, D., Bras, J., & Dufresne, A. (2010). Starch nanoparticles: A review. *Biomacromolecules,*
818 *11*, 1139-1153.
819 Leeman, A. M., Karlsson, M. E., Eliasson, A. C., & Bjorck, I. M. E. (2006). Resistant starch
820 formation in temperature treated potato starches varying in amylose/amylopectin ratio.
821 *Carbohydrate Polymers, 65*, 306-313.
822 Leloup, V. M., Colonna, P., Ring, S. G., Roberts, K., & Wells, B. (1992). Microstructure of amylose
823 gels. *Carbohydrate Polymers, 18*, 189-197.
824 Liao, K. S., Chen, H. M., Awad, S., Yuan, J. P., Hung, W. S., Lee, K. R., Lai, J. Y., Hu, C. C., &
825 Jean, Y. C. (2011). Determination of free-volume properties in polymers without
826 orthopositronium components in positron annihilation lifetime spectroscopy.
827 *Macromolecules, 44*, 6818-6826.
828 Lin, A. H. M., Nichols, B. L., Quezada-Calvillo, R., Avery, S. E., Sim, L., Rose, D. R., Naim, H. Y.,
829 & Hamaker, B. R. (2012). Unexpected high digestion rate of cooked starch by the Ct-
830 maltase-glucoamylase small intestine mucosal alpha-glucosidase subunit. *PLoS ONE, 7*,
831 e35473.
832 Liu, H. H., Chaudhary, D., Roberts, J., Weed, R., Sullivan, J., & Buckman, S. (2012). The interaction
833 in sorbitol-plasticized starch bionanocomposites via positron annihilation lifetime
834 spectroscopy and small angle X-ray scattering. *Carbohydrate Polymers, 88*, 1172-1176.
835 Lopez-Rubio, A., Flanagan, B. M., Shrestha, A. K., Gidley, M. J., & Gilbert, E. P. (2008). Molecular
836 rearrangement of starch during in vitro digestion: Toward a better understanding of enzyme
837 resistant starch formation in processed starches. *Biomacromolecules, 9*, 1951-1958.
838 Lopez-Rubio, A., Htoon, A., & Gilbert, E. P. (2007). Influence of extrusion and digestion on the
839 nanostructure of high-amylose maize starch. *Biomacromolecules, 8*, 1564-1572.

840 Menten, L., & Michaelis, M. I. (1913). Die kinetik der invertinwirkung. *Biochemistry, 49*, 333–369.
841 Miles, M. J., Morris, V. J., Orford, P. D., & Ring, S. G. (1985). The roles of amylose and
842 amylopectin in the gelation and retrogradation of starch. *Carbohydrate Research, 135*, 271-
843 281.
844 Montesanti, N., Veronese, G., Buleon, A., Escalier, P. C., Kitamura, S., & Putaux, J. L. (2010). A-
845 type crystals from dilute solutions of short amylose chains. *Biomacromolecules, 11*, 3049-
846 3058.
847 Morris, V. J., Gunning, A. P., Faulds, C. B., Williamson, G., & Svensson, B. (2005). AFM images of
848 complexes between amylose and Aspergillus niger glucoamylase mutants, native, and mutant
849 starch binding domains: A model for the action of glucoamylase. *Starch-Starke, 57*, 1-7.
850 Norouzian, D., Akbarzadeh, A., Scharer, J. M., & Young, M. M. (2006). Fungal glucoamylases.
851 *Biotechnology Advances, 24*, 80-85.
852 Oates, C. G. (1997). Towards an understanding of starch granule structure and hydrolysis. *Trends in*
853 *Food Science & Technology, 8*, 375-382.
854 Parchure, A. A., & Kulkarni, P. R. (1997). Effect of food processing treatments on generation of
855 resistant starch. *International Journal of Food Sciences and Nutrition, 48*, 257-260.
856 Pfannemüller, B. (1987). Influence of chain length of short monodisperse amyloses on the formation
857 of A-and B-type X-ray diffraction patterns. *International Journal of Biological*
858 *Macromolecules, 9*, 105-108.
859 Ramasubbu, N., Paloth, V., Luo, Y. G., Brayer, G. D., & Levine, M. J. (1996). Structure of human
860 salivary alpha-amylase at 1.6 angstrom resolution: Implications for its role in the oral cavity.
861 *Acta Crystallographica Section D-Biological Crystallography, 52*, 435-446.
862 Ring, S. G., I'Anson, K. J., & Morris, V. J. (1985). Static and dynamic light-scattering studies of
863 amylose aolutions. *Macromolecules, 18*, 182-188.
864 Robyt, J. F. (1986). Enzymes in the hydrolysis and synthesis of starch. In R. L. Whistler, J. N.
865 BeMiller & E. F. Paschall (Eds.), *Starch Chemisry and Technology (Second Edition)* (pp. 87-
866 123): Academic Press, Inc.
867 Robyt, J. F. (2009). Enzymes and their action on starch. In J. N. BeMiller & R. L. Whistler (Eds.),
868 *Starch chemistry and technology (Third edition)* (pp. 237-292): Academic press.
869 Robyt, J. F., & French, D. (1967). Multiple attack hypothesis of alpha-amylase action - Action of
870 porcine pancreatic human salivary and Aspergillus Oryzae alpha-amylases. *Archives of*
871 *Biochemistry and Biophysics, 122*, 8-16.
872 Robyt, J. F., & French, D. (1970). Action pattern of porcine pancreatic alpha-amylase in relationship
873 to substrate binding site of enzyme. *Journal of Biological Chemistry, 245*, 3917-3927.

874 Seneviratne, H., & Biliaderis, C. (1991). Action of α-amylases on amylose-lipid complex
875 superstructures. *Journal of Cereal Science, 13*, 129-143.
876 Shrestha, A. K., Ng, C. S., Lopez-Rubio, A., Blazek, J., Gilbert, E. P., & Gidley, M. J. (2010).
877 Enzyme resistance and structural organization in extruded high amylose maize starch.
878 *Carbohydrate Polymers, 80*, 699-710.
879 Singh, J., Dartois, A., & Kaur, L. (2010). Starch digestibility in food matrix: a review. *Trends in*
880 *Food Science & Technology, 21*, 168-180.
881 Slade, L., & Levine, H. (1987). Recent advances in starch retrogradation. *Industrial polysaccharides:*
882 *The impact of biotechnology and advanced methodologies*, 387-430.
883 Sorimachi, K., LeGalCoeffet, M. F., Williamson, G., Archer, D. B., & Williamson, M. P. (1997).
884 Solution structure of the granular starch binding domain of Aspergillus niger glucoamylase
885 bound to beta-cyclodextrin. *Structure, 5*, 647-661.
886 Swanson, S. J., Emery, A., & Lim, H. C. (1977). Kinetics of maltose hydrolysis by glucoamylase.
887 *Biotechnology and Bioengineering, 19*, 1715-1718.
888 Takahashi, T., Kato, K., Ikegami, Y., & Irie, M. (1985). Different behavior towards raw starch of 3
889 forms of glucoamylase from a Rhizopus Sp. *Journal of Biochemistry, 98*, 663-671.
890 Tester, R. F., & Debon, S. J. J. (2000). Annealing of starch: A review. *International Journal of*
891 *Biological Macromolecules, 27*, 1-12.
892 Tester, R. F., Karkalas, J., & Qi, X. (2004). Starch - composition, fine structure and architecture.
893 *Journal of Cereal Science, 39*, 151-165.
894 Thompson, D. B. (2000). Strategies for the manufacture of resistant starch. *Trends in Food Science*
895 *& Technology, 11*, 245-253.
896 Topping, D. L., Bajka, B. H., Bird, A. R., Clarke, J. M., Cobiac, L., Conlon, M. A., Morell, M. K., &
897 Toden, S. (2008). Resistant starches as a vehicle for delivering health benefits to the human
898 large bowel. *Microbial Ecology in Health and Disease, 20*, 103-108.
899 Tufvesson, F., Skrabanja, V., Björck, I., Elmståhl, H. L., & Eliasson, A.-C. (2001). Digestibility of
900 starch systems containing amylose–glycerol monopalmitin complexes. *Lwt-Food Science and*
901 *Technology, 34*, 131-139.
902 Tufvesson, F., Wahlgren, M., & Eliasson, A. C. (2003a). Formation of amylose-lipid complexes and
903 effects of temperature treatment. Part 1. Monoglycerides. *Starch-Starke, 55*, 61-71.
904 Tufvesson, F., Wahlgren, M., & Eliasson, A. C. (2003b). Formation of amylose-lipid complexes and
905 effects of temperature treatment. part 2. Fatty acids. *Starch-Starke, 55*, 138-149.

Van Munster, I. P., Tangerman, A., & Nagengast, F. M. (1994). Effect of resistant starch on colonic fermentation, bile-acid metabolism, and mucosal proliferation. *Digestive Diseases and Sciences, 39*, 834-842.

Warren, F. J., Butterworth, P. J., & Ellis, P. R. (2012). Studies of the effect of maltose on the direct binding of porcine pancreatic alpha-amylase to maize starch. *Carbohydrate Research, 358*, 67-71.

Warren, F. J., Zhang, B., Waltzer, G., Gidley, M. J., & Dhital, S. (2014). The interplay of α-amylase and amyloglucosidase activities on the digestion of starch in in vitro enzymic systems. *Carbohydrate Polymers,* Accepted for publication.

Weill, C. E., Burch, R. J., & Vandyk, J. W. (1954). An alpha-amyloglucosidase that produces beta-glucose. *Cereal Chemistry, 31*, 150-158.

Yuryev, V. P., Krivandin, A. V., Kiseleva, V. I., Wasserman, L. A., Genkina, N. K., Fornal, J., Blaszczak, W., & Schiraldi, A. (2004). Structural parameters of amylopectin clusters and semi-crystalline growth rings in wheat starches with different amylose content. *Carbohydrate Research, 339*, 2683-2691.

Zavareze, E. d. R., & Dias, A. R. G. (2011). Impact of heat-moisture treatment and annealing in starches: A review. *Carbohydrate Polymers, 83*, 317-328.

Zhang, B., Dhital, S., Flanagan, B. M., & Gidley, M. J. (2014). Mechanism for starch granule ghost formation deduced from structural and enzyme digestion properties. *Journal of Agricultural and Food Chemistry, 62*, 760-771.

Zhang, B., Dhital, S., & Gidley, M. J. (2013). Synergistic and antagonistic effects of α-amylase and amyloglucosidase on starch digestion. *Biomacromolecules, 12*, 1945-1954.

Zhang, B., Huang, Q., Luo, F. X., & Fu, X. (2012). Structural characterizations and digestibility of debranched high-amylose maize starch complexed with lauric acid. *Food Hydrocolloids, 28*, 174-181.

Zhang, B., Huang, Q., Luo, F. X., Fu, X., Jiang, H. X., & Jane, J. L. (2011). Effects of octenylsuccinylation on the structure and properties of high-amylose maize starch. *Carbohydrate Polymers, 84*, 1276-1281.

Zhang, B., Wang, K., Hasjim, J., Li, E. P., Flanagan, B. M., Gidley, M. J., & Dhital, S. (2014). Freeze-drying changes the structure and digestibility of B-polymorphic starches. *Journal of Agricultural and Food Chemistry, 62*, 1482-1491.

Zhang, G. Y., Ao, Z., & Hamaker, B. R. (2006). Slow digestion property of native cereal starches. *Biomacromolecules, 7*, 3252-3258.

939 Zobel, H. F. (1988a). Molecules to granules: A comprehensive starch review. *Starch/Starke, 40,* 44-
940 50.
941 Zobel, H. F. (1988b). Starch crystal transformations and their industrial importance. *Starch/Starke,*
942 *40,* 1-7.
943
944

945 Figure Captions

946

947 Figure 1. Digestion profiles and fitting plots of raw and cooked wheat and pea starches. Notes:
948 Digestion profiles of raw and cooked wheat (A) and pea (B) starches; Fitting plots for raw wheat (C),
949 raw pea (D), cooked wheat (E), and cooked pea (F) starches (Butterworth, et al., 2012).

950

951 Figure 2. Conformational changes occurring during retrogradation (Colonna, Leloup, & Buleon,
952 1992).

953

954 Figure 3. Kinetics of enzyme-resistant starch formation during wheat starch retrogradation at
955 different temperatures (0, 68 and 100 ^{o}C) as a function of time (A, first 200 min; B, extended time
956 period) (Eerlingen, Crombez, et al., 1993).

957

958 Figure 4. Enzyme-resistant starch levels compared with crystallinity from X-ray diffraction for
959 arrange of high amylose maize samples (Htoon, et al., 2009). (H, Hylon 7 starch; G, Gelose80
960 starch; R, raw starch; M, mild processed; E, extreme peocessed; RS, isolated resistant starch fraction).

961

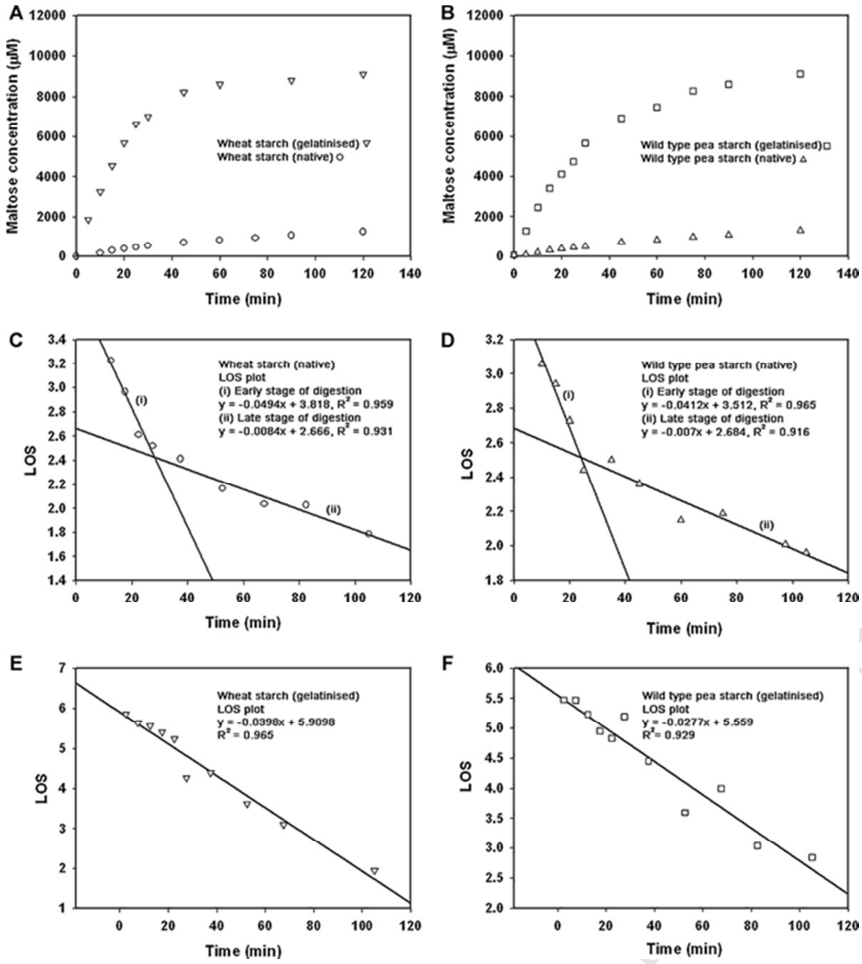

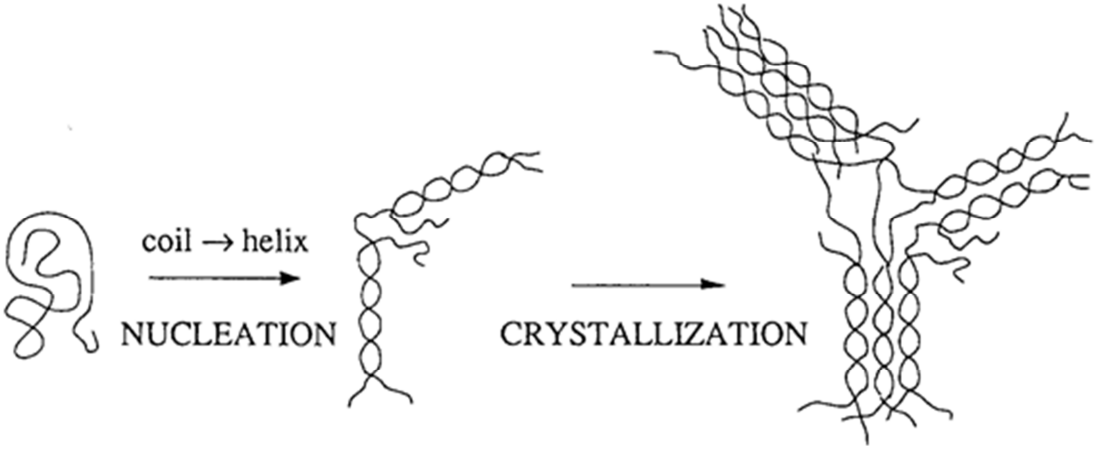

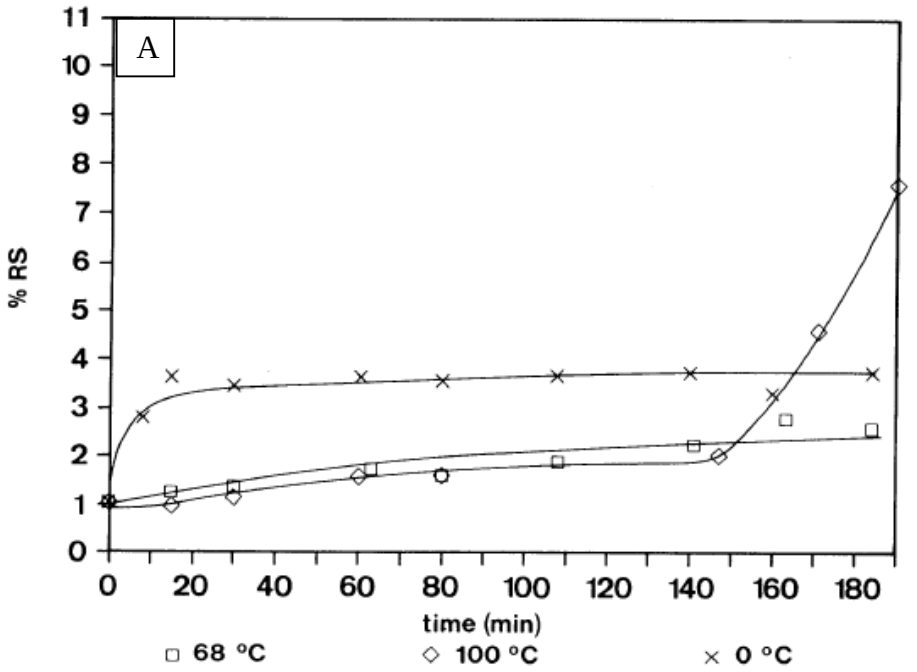
A
% RS
time (min)
□ 68 °C
◇ 100 °C
× 0 °C

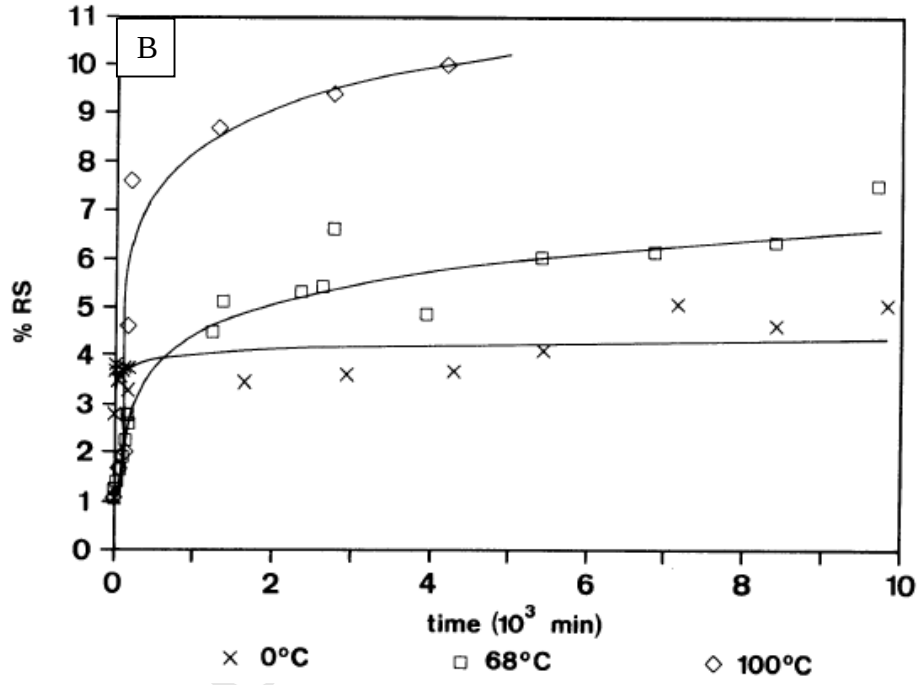
B
% RS
time (10³ min)
× 0°C
□ 68°C
◇ 100°C

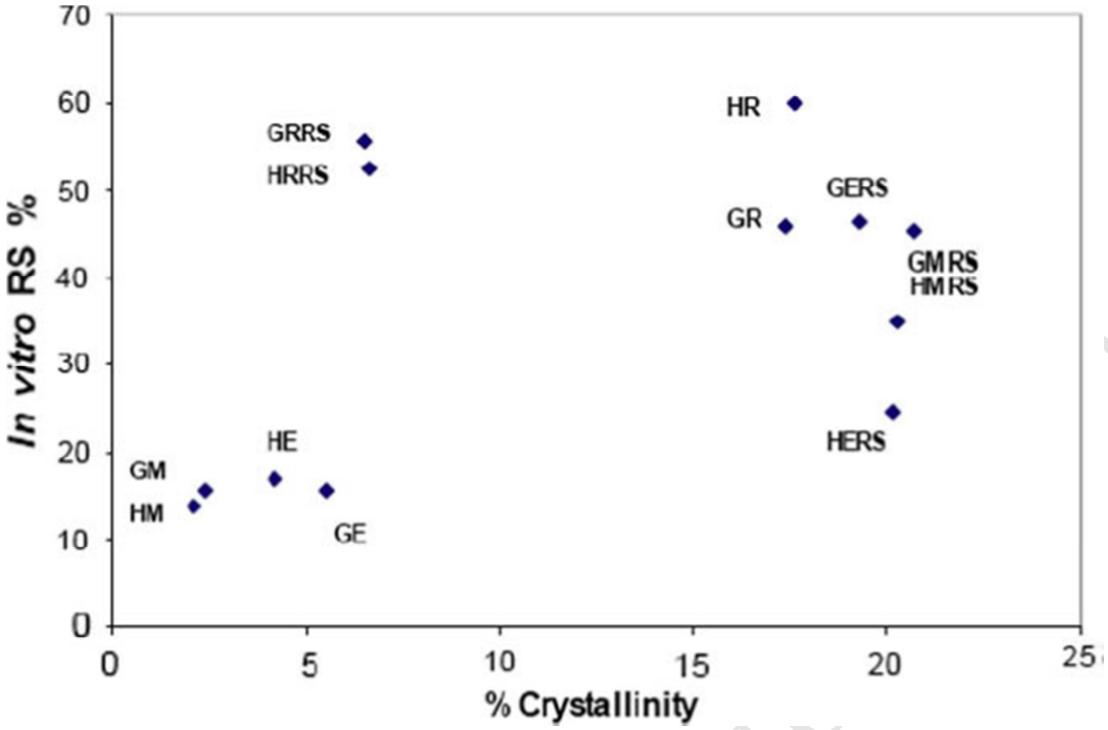

Highlights

- Rate limiting step in starch digestion controls levels of amylase resistance.
- Local starch molecular density major rate-controlling structural feature.
- High density achieved by (re-)crystallization or dense amorphous packing